THE JOURNAL OF BIOLOGICAL CHEMISTRY Vol. 279, No. 35, Issue of August 27, pp. 36828–36840, 2004

Printed in U.S.A.

RORα Regulates the Expression of Genes Involved in Lipid Homeostasis in Skeletal Muscle Cells

CAVEOLIN-3 AND CPT-1 ARE DIRECT TARGETS OF ROR*

Received for publication, May 4, 2004, and in revised form, June 8, 2004
Published, JBC Papers in Press, June 15, 2004, DOI 10.1074/jbc.M404927200

Patrick Lau‡§, Susan J. Nixon‡¶, Robert G. Parton‡¶‖, and George E. O. Muscat‡§‖‡‡**

From the ‡Institute for Molecular Bioscience, §Division of Molecular Genetics and Development, ¶Centre for Microscopy and Microanalysis, School of Biomedical Sciences, University of Queensland, St. Lucia, Queensland 4072, Australia

The *staggerer* mice carry a deletion in the RORα gene and have a prolonged humoral response, overproduce inflammatory cytokines, and are immunodeficient. Furthermore, the *staggerer* mice display lowered plasma apoA-I/-II, decreased plasma high density lipoprotein cholesterol and triglycerides, and develop hypo-α-lipoproteinemia and atherosclerosis. However, relatively little is known about RORα in the context of target tissues, target genes, and lipid homeostasis. For example, RORα is abundantly expressed in skeletal muscle, a major mass peripheral tissue that accounts for ~40% of total body weight and 50% of energy expenditure. This lean tissue is a primary site of glucose disposal and fatty acid oxidation. Consequently, muscle has a significant role in insulin sensitivity, obesity, and the blood-lipid profile. In particular, the role of RORα in skeletal muscle metabolism has not been investigated, and the contribution of skeletal muscle to the ROR−/− phenotype has not been resolved. We utilize ectopic dominant negative RORα expression in skeletal muscle cells to understand the regulatory role of RORs in this major mass peripheral tissue. Exogenous dominant negative RORα expression in skeletal muscle cells represses the endogenous levels of RORα and -γ mRNAs and ROR-dependent gene expression. Moreover, we observed attenuated expression of many genes involved in lipid homeostasis. Furthermore, we show that the muscle carnitine palmitoyltransferase-1 and caveolin-3 promoters are directly regulated by ROR and coactivated by p300 and PGC-1. This study implicates RORs in the control of lipid homeostasis in skeletal muscle. In conclusion, we speculate that ROR agonists would increase fatty acid catabolism in muscle and suggest selective activators of ROR may have therapeutic utility in the treatment of obesity and atherosclerosis.

Members of the nuclear hormone receptor (NR)[1] superfamily bind specific DNA elements and function as transcriptional regulators (1, 2). This group includes the "orphan NRs," which have no known ligands in the "classical sense." The orphan receptor, ROR/RZR (retinoic acid receptor-related orphan receptor), is closely related to Rev-erbAα, RVR/Rev-erbβ/BD73, and the *Drosophila* orphan receptor, E75A, particularly in the DNA-binding domain and the putative ligand-binding domain. ROR, Rev-erbAα, and RVR bind as monomers to an asymmetric $(A/T)_6$RGGTCA motif. ROR functions as a constitutive transactivator of gene expression, and in contrast, Rev-erbAα and RVR do not activate transcription, mediate transcriptional repression, and can repress constitutive trans-activation from this motif by RORα (3–9).

Three ROR/RZR genes have been identified; RORα encodes four RORα isoforms α1, α2, α3, and RZRα, which are alternatively spliced products of the RORα gene and are predominantly expressed in blood, brain, skeletal muscle, and fat cells (8, 10). RORβ/RZRβ is expressed specifically in the brain (11), and RORγ is found at high levels in skeletal muscle (12–14).

Genetic studies have implicated RORα in the regulation of lipid homeostasis. For example, analysis of RORα function has been assisted by a natural mutation in an obese mouse strain called *staggerer* (*sg*/*sg*). The mutation produces a dominant negative RORα that results in a functional knockout phenotype. In accordance with the wide expression pattern of RORα, *staggerer* mice show symptoms of ataxia and cerebellar dysfunction, susceptibility to atherosclerosis and hypo-α-lipoproteinemia, vascular dysfunction, muscular irregularities, osteoporosis, and severe immune abnormalities. In the context of lipid homeostasis, the *staggerer* mice exhibit an aberrant blood lipid profile with lower circulating plasma levels of HDL-C, apolipoprotein (apo) CIII, and plasma triglycerides. Decreases in specific lipoprotein compartments, namely apoAI, the major constituent of HDL, and apoAII, leads to a pronounced hypo-α-lipoproteinemia (16). Accordingly, it has been shown that RORα regulates the expression of apoAI and apoCIII in cell culture (16, 17). Susceptibility to atherosclerosis in this animal model is linked to a complex phenotype that includes aberrant vascular physiology, lipid profiles, and hypersensitive inflammatory responses.

Studies examining motor capabilities and coordination in *staggerer* mice have shown a reduction of muscular strength in these mice (18). Furthermore, the studies of Lau *et al.* (19) demonstrated that RORα potentiates skeletal muscle myogen-

* This work was supported in part by a National Health and Medical Research Council of Australia project grant. The costs of publication of this article were defrayed in part by the payment of page charges. This article must therefore be hereby marked "*advertisement*" in accordance with 18 U.S.C. Section 1734 solely to indicate this fact.

‖ Principal Research Fellow of the National Health and Medical Research Council of Australia.

** Supported by the National Health and Medical Research Council of Australia and the National Heart Foundation of Australia.

‡‡ To whom correspondence should be addressed. Tel.: 61-7-3346-2039; E-mail: g.muscat@imb.uq.edu.au.

[1] The abbreviations used are: NR, nuclear hormone receptor; HDL, high density lipoprotein; LXR, liver X receptor; PPAR, peroxisome proliferator-activated receptor; DMEM, Dulbecco's modified Eagle's medium; LUC, luciferase; Q-RT, quantitative real time; GAPDH, glyceraldehyde-3-phosphate dehydrogenase; oligo, oligonucleotide; EMSA, electrophoretic mobility shift analysis; GST, glutathione S-transferase; SREBP, sterol regulatory element binding protein; LPL, lipoprotein lipase; FABP, fatty acid binding protein; FAS, fatty-acid synthase; tk, thymidine kinase; CAT, chloramphenicol acetyltransferase; ADRP, adipophilin/adipocyte differentiation-related protein; Cav, caveolin.

esis, and the comments in a review by Jarvis *et al.* (20) suggest that *staggerer* mice have skeletal muscle irregularities.

The association between RORα, lipid homeostasis, and skeletal muscle is not surprising. RORα is abundantly expressed in skeletal muscle, which is one of the most metabolically demanding tissues that relies heavily on fatty acids as an energy source and accounts for 75% of glucose disposal. Moreover, this suggests that muscle has an important role in obesity, which is primarily controlled by increased food intake or decreased energy expenditure. However, the fundamental role of RORα in skeletal muscle cholesterol, lipid, glucose, and energy homeostasis has not been examined. Moreover, the contribution of skeletal muscle, a major mass tissue, to the ROR knockout phenotype has not been resolved.

The involvement of RORα in the progression of atherosclerosis identifies RORα as a therapeutic target in the treatment of cardiovascular disease. In addition, skeletal muscle is rapidly emerging as a critical target tissue in the battle against obesity, type II diabetes, dyslipidemia, syndrome X, and atherosclerosis. NRs in skeletal muscle, for example liver X receptor (LXR), peroxisome proliferator-activated receptors (PPAR) α, β/δ, and γ, have been shown to be involved in enhancing insulin-stimulated glucose disposal rate, decreasing triglycerides and increasing lipid catabolism, cholesterol efflux, and plasma HDL-C levels (21–23). Hence, orphan NRs that regulate lipid and glucose metabolism, cholesterol homeostasis, energy expenditure, and thermogenesis in skeletal muscle have enormous pharmacological utility for the treatment of dyslipidemia and syndrome X.

We hypothesize that RORα regulates lipid, glucose, and energy homeostasis in this major mass lean tissue. This hypothesis was addressed by examining the effect of ectopically expressing the *staggerer* form of RORα in muscle cells and by investigating the subsequent effect on gene expression involved in lipid metabolism. Our investigation reveals that ROR has a central role in the regulation of lipid metabolism in muscle cells. Moreover, we suggest that the atherogenic and dyslipidemic phenotype of the *staggerer* mouse is related to aberrant RORα function in skeletal muscle.

MATERIALS AND METHODS

Cell Culture—Mouse myogenic C2C12 cells were cultured in growth medium (DMEM supplemented with 10% Serum Supreme (BioWhittaker, Edward Keller Pty. Ltd., Hallam, Victoria, Australia)) in 6% CO_2. Myoblasts were differentiated into post-mitotic multinucleated myotubes by 1–5 days of serum withdrawal (*i.e.* cultured in DMEM supplemented with 2% horse serum). Cells were harvested at indicated time points, usually 120 h (5 days) after the mitogen withdrawal, unless indicated differently. African green monkey kidney COS-1 cells were grown in DMEM supplemented with 10% heat-inactivated fetal calf serum.

Transient Transfections—Each well of a 24-well plate of COS-1 cells (~60% confluence) was transfected with a total of ~0.6–0.8 μg of DNA per well by using the liposome-mediated transfection procedure as described previously (19). Cells were transfected using an *N*-[1-(2,3-dioleoyloxy)propyl]-*N,N,N*-trimethylammonium methylsulfate and Metafectene (Biontex Laboratories GmbH, Munich, Germany) liposome mixture in 1× HBS (HEPES-buffered saline (42 mM HEPES, 275 mM NaCl, 10 mM KCl, 0.4 mM Na_2HPO_4, 11 mM dextrose (pH 7.1)). The DNA/*N*-[1-(2,3-dioleoyloxy)propyl]-*N,N,N*-trimethylammonium methylsulfate/Metafectene mixture was added to the cells in 0.5–0.6 ml of DMEM supplemented with 5% charcoal-stripped fetal calf serum. 16–24 h later, the culture medium was changed, and the cells were subsequently harvested for the assay of luciferase activity 24–48 h after the transfection period as described previously. Fold activation is expressed relative to LUC activity obtained after cotransfection of the reporter and pSG5 vector only, arbitrarily set at 1. The mean fold activation values and standard deviations were derived from a minimum of two independent experiments composed of six replicates. CAT assays were described previously (19). Transient transfections were performed at least twice in sextuplicate.

C2C12 Stable Transfection—Myogenic C2C12 cells, cultured in growth medium, were cotransfected with pSG5-RORΔDE (and pCMV-NEO at a 20:1 ration of expression vector/NEO vector) by the liposome-mediated procedure in duplicate. The cells were then grown for another 24 h to allow cell recovery and neomycin resistance expression before G418 selection. After 10–14 days selection with 450 μg/ml G418 (Invitrogen) in culture medium, the two independent polyclonal pools (>100 colonies per pool) of stable transfectants were cultured and maintained on 200 μg/ml G418 medium.

RNA Extraction—Total RNA was extracted from C2C12 using TRI-Reagent (Sigma), according to manufacturer's protocol. RNA for quantitative real time (Q-RT)-PCR, was further purified by using RNeasy (Qiagen, Clifton Hill, Victoria, Australia), according to manufacturer's instructions. This was followed by DNase treatment with DNA-free (Ambion, Austin, TX.)

Q-RT-PCR—RNA was normalized using UV spectrophotometry and agarose gel electrophoresis. Complementary DNA was synthesized from 7 μg of total RNA by Superscript3, according to the manufacturer's instruction (Invitrogen). Target cDNA levels were analyzed by Q-RT-PCR in 25-μl reactions containing either 1× SYBR green (ABI, Warrington, UK) or Taqman PCR master mix (ABI, Branchburg, NJ), 200 nM each forward and reverse primers or Assay on Demand Taqman primers (ABI, Foster City, CA) and cDNA (0.6% of the starting 7 μg of RNA) by using an ABI Prism 7000 Sequence Detector system. PCR was conducted over 45 cycles of 95 °C for 15 s and 60 °C for a 1-min two-step thermal cycling preceded by an initial 95 °C for 10 min for activation of Amplitaq Gold DNA polymerase.

Primers—The *Mus musculus* primer sequences (forward and reverse, respectively) used are as follows: ABCA1, GCTCTCAGGTGGGATGCAG and GGCTCGTCCAGAATGACAAC; 18 S, GATCCATTGGAGGGCAAGTCT and CCAAGATCCAACTACGAGCTTTTT; A8/G1, CTGAGGGATCTGGGTCTGA and CCTGATGCCACTTCCATGA; ACS4, GGTTTGGTAACAGATGCCTTCAA and CCCATACATTCGCTCAATGTCTT; ADRP, CCCTGGTTCTAAGAAGCTGCTTT and GGCCAGATGACCCCTTTTG; AdipoR1, ACGTTGGAGAGTCATCCCGTAT and CTCTGTGTGGATGCGGAAGAT; AdipoR2, TCCCAGGAAGATGAAGGGTTTAT and TTCCATTCGTTCGATAGCATGA; apoE, GCTGTTGGTCACATTGCTGA and TGCCACTCGAGCTGATCTG; β-actin, GCTCTGGCTCCTAGCACCAT and CCACCGATCCACACAGAGTAC; CD36, GGCCAAGCTATTGCGACAT and CAGATCCGAACACAGCGTAGA; CAV-3, CTGCCCCCAGGACTATCAAC and TTCCAGATCCGTGTGCTCTTC; CPT1b, ATCATGTATCGCCGCAAACT and CCATCTGGTAGGAGCACATGG; FABP3, CCCCTCAGCTCAGCACCAT and CAGAAAAATCCCAACCCAAGAAT; FAS, CGGAAACTTCAGGAAATGTCC and TCAGAGACGTGTCACTCCTGG; GAPDH, GTGTCCGTCGTGGATCTGA and CCTGCTTCACCACCTTCTTG; Glut4n ATGGCTGTCGCTGGTTTCTC and ACCCATACGATCCGCAACAT; Glut5, CTTGCCTTTACCGGGTTGAC and CATCTGGTCTTGCAGCAACTCT; MyoG, CCTTAAAGCAGAGAGCATCC and GGAATTCGAGGCATAATATGA; LPL, CCAATGGAGGCACTTTCCA and TGGTCCACGTCTCCGAGTC; mRORα, CAATGCCACCTACTCCTGTCC and GCCAGGCATTTCTGCAGC; PGC-1, CGATGTGTCGCCTTCTTGCT and CGAGAGCGCATCCTTTGG; Rev-erb, CCACACCGCTGGGAGAGT and GCCCTGGCGTAGACCATTC; RVR, GGAAACACTCATCCGTGCACTA and ATCGAAGATCTGGCAACTTTAGAA; SCD-1, TGTACGGGATCATACTGGTTCC and CCCGGCTGTGATGCC; SCD-2, ACTGTGACTCAAGTTCAACTCTTGAAA and TGCCCACAAATTGAGGATAGC; and SREBP-1c, CGTCTGCACGCCCTAGG and CTGGAGCATGTCTTCAAATGTG; TNNI1, GCCTATGCGCACACCTTTG and CGGGTACCATAAGCCCACACT; TNNI2, AAATGTTCGAGTCTGAGTCCTAACTG and GCCAAGTACTCCCAGACTGGAT; UCP-2, GTTCCTCTGTCTCGTCTTGC and GGCCTTGAAACCAACCA; and UCP-3, TGACCTGCGCCCAGC and CCCAGGCGTATCATGGCT.

Human RORα-specific primers contain 3 of 5 base difference at the 3′ end of the reverse primer relative to mouse primers. hRORα: CAATGCCACCTACTCCTGTCC and CTACGGCAAGGCATTTCTGTAAT. GAPDH and 18 S were used for normalization between samples for quantitation. Assay on Demand primers were used for Taqman real time PCR (ABI, Foster City CA) m+hROR (Mm00443103_m1); RORγ (Mm00441139_m1); FABP4 (Mm00445880_m1); GAPDH (Mm99999915_g1); 18 S rRNA (Hs99999901_s1).

Plasmids—Human pSG5-RORα1 has been previously described (19). ROREx5-tk-LUC containing five copies of RORE (TATATCAAGGTCAT) was cloned into pTKLuc as described by Medvedev *et al.* (24). mPCP-2x4-tk-LUC containing four copies of mouse Pcp-2 RORE (GTTATAGTAACTGGGTCAGGGGACT) was cloned into pTKLuc as described by Matsui (25). The inserted sequences in the TKLuc clones were confirmed by big dye terminator version 3.1 cycle sequencing

(ABI, Foster City, CA). The CPT-1 promoter (−1025/−12) was kindly provided by D. P. Kelly (26); cDNA-GRIP1/SRC2 and cDNA-p300 have been described previously (27). CDNA4-PGC-1 was kindly provided by Spiegelman and co-workers (28). 2.6-kb mouse caveolin-3 promoter was isolated from a BAC clone 23N20 (Incyte Genetics) and cloned into a HindIII site of pGL3basic. Deletion constructs of the Cav-3 promoter were obtained using native restriction sites or by PCR with *Pfu* DNA polymerase. The DNA sequences of these constructs were confirmed by cycle sequencing (Applied Biosystems). GLUT4-pGL2 was obtained by PCR cloning of a mouse skeletal muscle genomic DNA into pGL2basic. The DNA sequence containing a 2.2-kb sequence upstream of the transcription start site was confirmed by cycle sequencing. pGEX-RORα1 was described previously (19); GAL4-ROR constructs were cloned in-frame into the multiple cloning site of vector pGAL0 and confirmed by dideoxy sequencing (Amersham Biosciences).

Site-directed Mutagenesis—pGL3-Cav3Luc (−2595/+35) was mutated by QuickChange PCR site-directed mutagenesis (Stratagene) according to the manufacturer's instructions. 125 ng of oligonucleotides containing GG to TT mutation and its complementary strand (see sequences below) were added to a PCR containing 50 ng of pGL3-Cav3Luc (−2595/+35), dNTP, 1× *Pfu* buffer, and *Pfu* or *Pfu* ultra. After restriction digestion with DpnI, the reaction was transformed into DH5α. The colonies were screened, and the sequence was confirmed by cycle sequencing after DNA extraction. The oligonucleotides to mutate the mouse caveolin-3 promoter are as follows: Cav-3 mut2 oligos, GAGGATACAATCTCGTGTCAAATACTCACCCGCCCCG and CGGGGCGGGTGAGTATTTGACACGAGATTGTATCCTC; and the Cav-3 mut6 oligos, CATGCGGCTCCCAGTGAAAGACTTCCTCCTCTCGAG and CTCGAGAGGAGGAAGTCTTTCACTGGGAGCCGCATG.

Oligonucleotide Probes and EMSA—Double-stranded oligonucleotide probes used in EMSA and for cold competition are as follows: RORE, 5′-TCGACTCGTATATCAAGGTCAAGCGTG-3′ (8); mouse pcp-2, 5′-GTTATAGTAACTGGGTCAGGGGACTC-3′ (25); Cav-3 m1, CTGAGAACTACGTCATGGCCTTTG; Cav-3 m2, CTCGTGTCACCTACTCACCCG; Cav-3 m3, CTGCTCCAAGGCACAGGAGAGCAGAGC; Cav-3 m4, AGCAGAGCAAGGTCTTTGTCCCTTTGGTGTC; Cav-3 m5, CATGGACAAGGTAAAGGGGAGGCTTATAACTG; and Cav-3 m6, CCAGTGACCGACTTCCTCCTCT.

GST-RORα1 was prepared as previously described (19, 52). 100 ng of double-stranded oligonucleotide was radiolabeled with 5 μl of [γ-^{32}P]ATP and T4 polynucleotide kinase and purified by 6% TBE-PAGE.

EMSAs were carried out as described previously with modifications (52, 55). 0.4 μg of GST-RORα1 protein in Dignam buffer C (0.1 M NaCl, 20 mM HEPES (pH 7.9), 2 mM EDTA, 1 mM dithiothreitol, and 1× complete protease inhibitor (Roche Applied Science)) was incubated with 1 μg of poly(dI-dC)·(dI-dC), 4 μg of bovine serum albumin, 1× complete protease inhibitor (Roche Applied Science), 300 cps of gel-purified ^{32}P double-stranded radioactive probe end-labeled by T4 polynucleotide kinase, 12% glycerol, 0.6 mM dithiothreitol, and 1× binding buffer (53) on ice for 30 min before gel separation. Cold competition studies were carried out by coincubation with 100–300 ng of double-stranded unlabeled probe.

RESULTS

RORα and -γ mRNA Expression Are Induced during Myogenic Differentiation—RORα and -γ mRNAs are expressed in skeletal muscle tissue. To elucidate the functional role of RORα in skeletal muscle, we initially investigated the expression of RORα mRNA relative to the 18 S rRNA in the mouse C2C12 myoblast cell line. This skeletal muscle cell line has proven to be a reliable system to study skeletal muscle lipid homeostasis in cell culture (21–23).

Proliferating C2C12 myoblasts can be induced to biochemically and morphologically differentiate into post-mitotic multinucleated myotubes by serum withdrawal in culture over a 48–96-h period. This transition from a non-muscle phenotype to a contractile phenotype is associated with the repression of non-muscle proteins and the activation/expression of a structurally diverse group of genes responsible for contraction and to cope with the extreme metabolic demands on this organ (Fig. 1*A*).

By using the GenBank™ sequences of RORα and -γ, we designed specific primers for the amplification of mouse ROR by quantitative real time PCR from total RNA isolated from proliferating and differentiated C2C12 cells (Fig. 1*A*). Total poly(A)$^+$ RNA was isolated from proliferating myoblasts (PMB), confluent myoblasts (CMB), and post-mitotic myotubes after 2 and 5 days (MT2 and MT5) of serum withdrawal and examined by real time PCR and "Northern blot" analysis.

We observed that RORα and -γ are expressed in proliferating myoblasts; however, these transcripts are induced 2.5–4-fold, relative to 18 S rRNA and GAPDH mRNA (data not shown), as the cells exit the cell cycle and fuse to form differentiated multinucleated myotubes that have acquired a muscle-specific phenotype (Fig. 1, *B* and *D*). RORα is seen transcribed as a double band (Fig. 1*C*) in C2C12 as described in differentiated P19 cells (3). Concomitant with this increase in ROR encoding mRNAs was the striking induction of myogenin mRNA (Fig. 1*E*), which encodes the hierarchical bHLH regulator, and repression of the cytoskeletal non-muscle β-actin mRNA (Fig. 1*F*), which confirmed that these cells had terminally differentiated. Moreover, we observed the induction of the slow and fast isoforms of the contractile protein, troponin I (Fig. 1, *G* and *H*). These data demonstrated that the RORα and -γ mRNA transcripts were expressed in C2C12 cells, and expression is increased upon myotube formation.

Induction of RORα and -γ mRNAs correlated with the repression of the mRNAs encoding the closely related but opposingly acting Rev-erbα and β(RVR) orphan nuclear receptors (Fig. 1, *I* and *J*), which are abundantly expressed in proliferating myogenic cells but are repressed during myogenic differentiation. This is in concordance with previous observations (50, 51).

Ectopic RORΔE Expression Represses Endogenous Levels of RORα and -γ and Attenuates ROR-dependent Gene Expression—To understand the biological role of RORα in skeletal muscle lipid homeostasis and to identify the metabolic target(s) of this orphan receptor in muscle cells, we proceeded to examine the effect of attenuating ROR function in C2C12 cells.

In order to perturb ROR function and to disrupt ROR-mediated gene expression, we utilized the RORΔDE plasmid. This construct encodes amino acids 1–235 but lacks the entire E region and part of the hinge/D region of RORα. This was chosen because McBroom *et al.* (30) reported that deletion of this region preserved DNA binding but destroyed trans-activation and operated in a dominant negative manner. Furthermore, the "*staggerer*" phenotype in mice is because of a frameshift mutation in RORα (29), which produces a similar nonfunctional C-terminal domain. Finally, we noted that GAL4 hybrid analysis indicated that the RORα activation domain was located downstream of amino acid position 235 (Fig. 2*A*). Moreover, in concordance with this observation, we demonstrated that RORΔDE (RORα1-(1–235)) ablated the ROR-mediated trans-activation of the synthetic (ROREx5) and native (mPCP-2 × 4) ROR-dependent response elements linked to the basal tk-LUC reporter (Fig. 2, *B* and *C*). Also shown is the opposingly acting RVR/rev-erb β orphan that does not trans-activate the ROREs. Moreover, the RORΔDE repressed the ROR-mediated trans-activation of the synthetic heterologous RORE-tk-LUC reporter in a dose-dependent manner, similar to the orphan receptor RVR (Fig. 2, *D* and *E*). This demonstrated that this construct, as expected from studies on the *staggerer* form of ROR and other forms of ROR that lack the entire E region and parts of the hinge, attenuated ROR-dependent gene expression.

We stably (and independently) cotransfected two populations of C2C12 cells with RORΔDE and pCMV-NEO expression vectors. Stable RORΔDE transfectants were isolated as two independent polyclonal pools of G418-resistant colonies (composed of >20 individually resistant colonies). The C2:RORΔDE cells

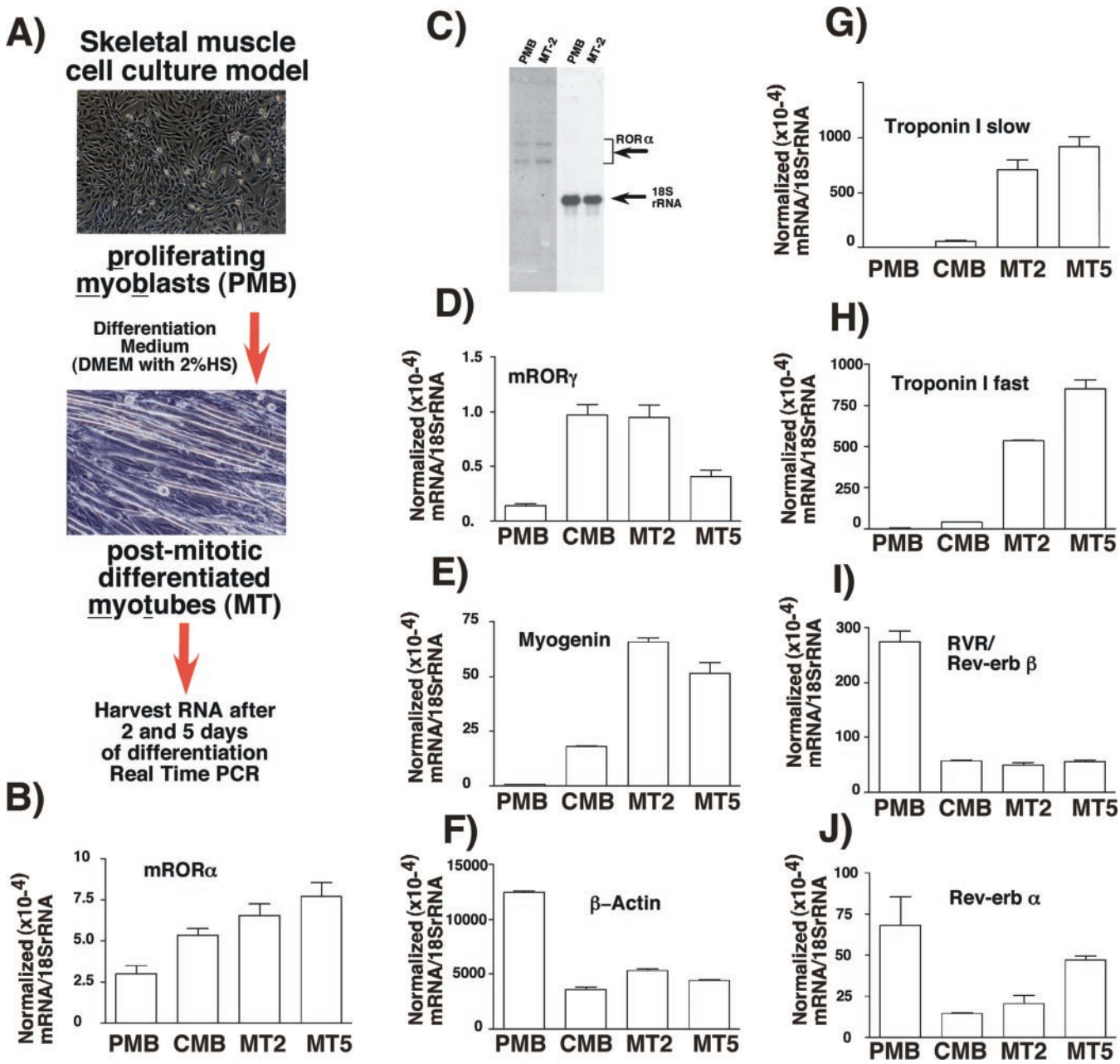

FIG. 1. **ROR mRNA expression in skeletal muscle cells.** *A*, schematic illustration of the cell culture model. Proliferating myoblasts are cultured in DMEM supplemented with 10% serum supreme. Myoblasts were differentiated into post-mitotic multinucleated myotubes by 1–5 days of serum withdrawal (*i.e.* cultured in DMEM supplemented with 2% horse serum). *B–J*, Q-RT-PCR analysis of RORα and -γ mRNA expression during skeletal myogenesis. Total RNA was extracted from C2C12 proliferating myoblasts (*PMB*), confluent myoblasts (*CMB*), and myotube (*MT*) after 2 days of serum withdrawal (*MT2*) and myotubes after 5 days of serum withdrawal (*MT5*), and 7 μg of each sample was reverse-transcribed to cDNA. Subsequently, 0.6% of the cDNA was analyzed by Q-RT-PCR (see "Materials and Methods"). *B*, Q-RT-PCR analysis of mRORα levels. *C*, Northern analysis of RORα mRNA levels as reported previously (19). Q-RT-PCR analyses of mRORγ mRNA levels (*D*); mRNA levels (MyoG) (*E*); β-actin mRNA levels (*F*); troponin I slow/type 1 (TNNI1) mRNA levels (*G*); troponin I fast/type II (TNNI2) mRNA levels (*H*); RVR mRNA levels (*I*); and Rev-erbα mRNA levels (*J*). (Primer sequences and experimental conditions for Q-RT-PCR are described under "Materials and Methods.") Levels of 18 S were measured in all samples, and the results were normalized and presented as number of target transcripts per 18 S transcript. For example β-actin is equivalently expressed to 18 S.

were transfected with pSG5-RORΔDE (*i.e.* amino acids 1–235). The two polyclonal pools of C2-RORα1-(1–235) cells abundantly expressed the ectopic/exogenous human transcript relative to GAPDH and 18 S rRNA controls. This was demonstrated rigorously by quantitative real time PCR with primers that specifically detect the human-specific transcript expressed from the expression vector (Fig. 3, *A* and *B*) and Northern analysis (Fig. 3*C*). Furthermore, the total pool size of RORα mRNA increased ~2–3-fold when measured by real time PCR with primers that detected both mouse and human transcripts (Fig. 3*D*). Most interestingly, we observed by real time PCR and Northern analysis that the endogenous levels of the mouse RORα mRNA transcripts were reduced in both polyclonal pools of the C2-RORα1-(1–235) cells (Fig. 3, *E* and *F*) relative to the wild type levels. The down-regulation of the endogenous RORα transcripts is not surprising. During myogenesis mRNA pool sizes in muscle tissue are under strict control (31), and mechanisms exist that sense total output from exogenous and endogenous genes (32). Furthermore, exogenous expression of a number of different contractile protein transgenes in the mouse (*e.g.* myosin light chain 2 and troponin I fast, skeletal, and cardiac actin) results in the decline in the expression of the

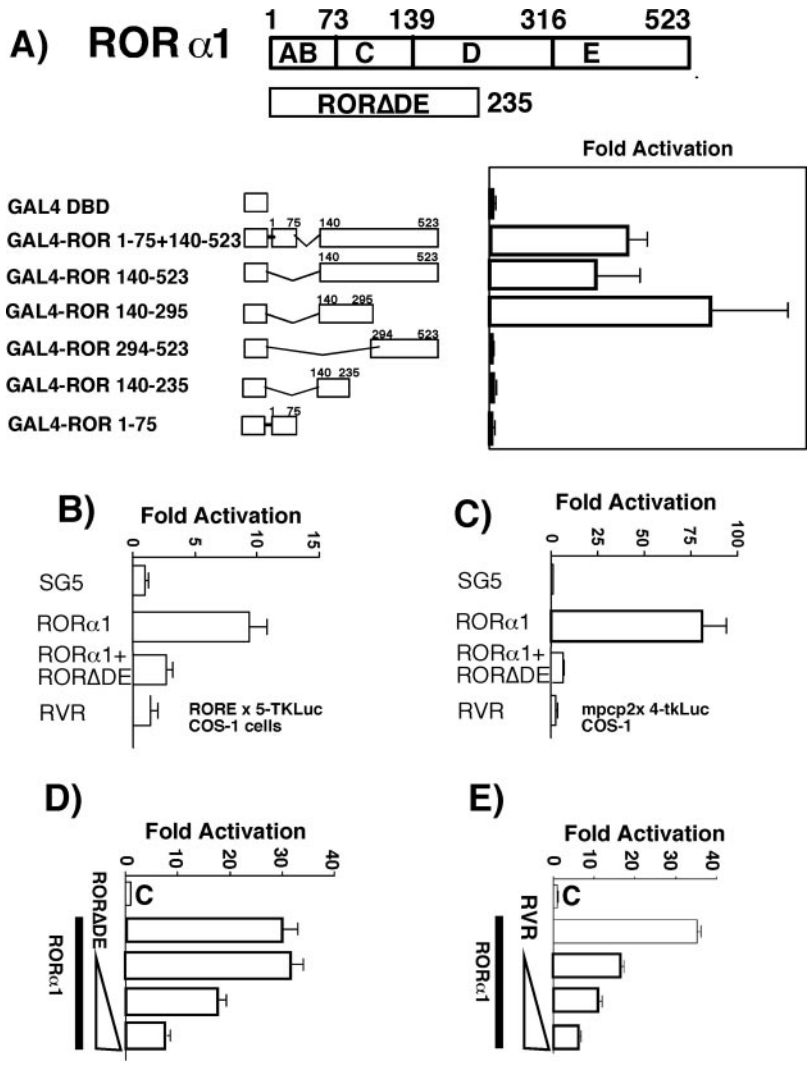

FIG. 2. **RORα-(1–235)/RORΔDE attenuates ROR-dependent gene expression.** *A*, diagrammatic representation of RORα and the Gal4-ROR chimeric constructs. Each well of a 6-well plate of COS-1 cells (~60% confluence) was cotransfected with 1.0 μg of the Gal4-ROR chimera and 3.0 μg of the GAL reporter G5Elb-CAT by the liposome-mediated transfection procedure as described under "Materials and Methods." Briefly, the DNA/liposome mix was added to the cells in 3 ml of DMEM supplemented with 5% charcoal-stripped fetal calf serum. 16–24 h later, the culture medium was changed, and the cells were subsequently harvested for the assay of CAT enzyme activity 24–48 h after the transfection period. Fold activation is expressed relative to CAT activity obtained after cotransfection of the Gal4 DNA-binding domain alone, arbitrarily set at 1. The mean fold activation values and S.D. (*bars*) were derived from a minimum of two independent triplicate experiments. *B*, each well of a 24-well plate of COS-1 cells (~60% confluence) was cotransfected with either 0.33 μg of the synthetic reporter, ROREx5-tk-LUC (the RORE sequences are described under "Materials and Methods"). Additionally, either 0.32 μg of pSG5, 0.16 μg each of pSG5-RORa and pSG5, 0.16 μg each of pSG5-RORa1 and pSG5-RORΔDE, or 0.16 μg each of pSG5-RORa and pSG5-RVR (*i.e.* a total of ~0.65 μg of DNA per well) used the liposome-mediated transfection procedure as described in *A*. Fold activation is expressed relative to LUC activity obtained after cotransfection of the reporter, and pSG5 vector only was arbitrarily set at 1. The mean fold activation values and S.D. (*bars*) were derived from a minimum of two independent experiments composed of six replicates. *C*, identical to *B*, except the native reporter, mPCP-2x4-tk-LUC, has been utilized. *D* and *E*, COS-1 cells were transiently transfected as above with 0.32 μg of the synthetic reporter, ROREx5-tk-LUC. The control transfection (*C*), arbitrarily set to 1, also contained 0.32 μg of the pSG5 vector alone. All the other transfections contained 0.16 μg of pSG5-RORa1 per well of a 24-well plate. Additionally, the three denoted transfections were cotransfected with increasing amounts (0.04, 0.08, and 0.16 μg) of pSG5-RORΔDE (*D*) and pSG5-RVR (*E*), respectively. The vector pSG5 was used to standardize the quantity of DNA to a total of ~0.65 μg of DNA per well. Fold activation is expressed relative to luciferase activity obtained after cotransfection of the reporter with the pSG5 vector alone, arbitrarily set at 1. The mean luciferase fold activation values and S.D. (*bars*) were derived from a minimum of 2–3 independent experiments composed of six replicates.

corresponding endogenous gene (32–36). Finally, we observed that ectopic expression of the RORαΔDE in muscle C2 cells completely ablated RORγ mRNA expression (Fig. 3*G*).

In conclusion, the cell lines ectopically expressed a dominant negative RORα expression vector that compromises ROR function and ROR-dependent gene expression. Moreover, RORα mRNA expression is attenuated, and RORγ mRNA expression is ablated.

ROR Regulates Lipid Homeostasis; Dominant Negative ROR Activity Represses the Expression of Genes Involved in Lipid Absorption, Utilization, and Efflux—We investigated the expression of the genes involved in skeletal muscle lipid and carbohydrate metabolism (see Table I) in the wild type and the RORΔDE-expressing C2C12 cells. This *in vitro* cell culture system has been used to investigate the regulation of cholesterol homeostasis and lipid metabolism by LXR agonists (22). Muscat *et al.* (22) demonstrated that the selective and synthetic liver X receptor (LXR) agonist, T0901317, induced similar effects on mRNAs encoding the ATP-binding cassette A1/G1 (ABCA1/G1), apolipoprotein E (apoE), stearoyl-CoA desaturase-1 (SCD-1), sterol regulatory element binding protein-1c (SREBP-1c), etc. in differentiated C2C12 myotubes and *M. musculus* quadriceps skeletal muscle tissue. Moreover, treatment of these cells with PPARα and -δ agonists and an

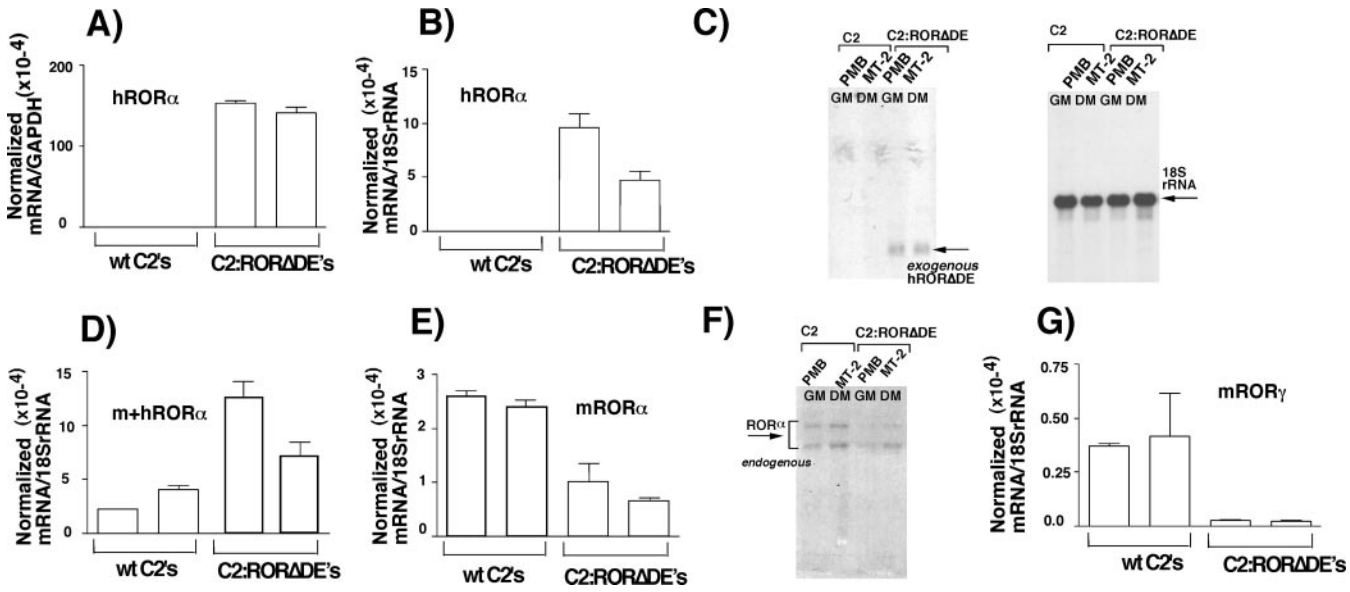

FIG. 3. **Q-RT-PCR analyses of the RORΔDE stably transfected C2C12 cell line.** Q-RT-PCR analysis of endogenous and exogenous/ectopic ROR mRNA expression in two independent populations of native/wild type (*wt*) differentiated mouse C2C12 cells and two independent polyclonal pools of the C2C12 cells were stably transfected with the dominant negative human RORa1ΔDE expression vector after 5 days of serum withdrawal. These cells were denoted as wild type C2s and C2:RORΔDE, respectively. *A*, Q-RT-PCR analysis of the dominant negative human RORα (*hROR*) mRNA expression in the two independent populations of wild type mouse C2C12 cells, and the two independently transfected polyclonal pools of the C2:RORΔDE cells relative to the GAPDH control. *B*, Q-RT-PCR analysis of hRORα mRNA expression relative to the 18 S rRNA control. *C*, Northern analysis of the dominant negative human RORα mRNA as reported previously (19). Total RNA from proliferating myoblasts (*PMB*) and myotubes after 2 days of serum withdrawal (*MT2*) was isolated from wild type and stably transfected cells. Subsequently, RNA was Northern-blotted and hybridized with a ^{32}P-labeled human ROR probe and an oligo that recognizes the 18 S rRNA. *D*, Q-RT-PCR analysis of total mouse + human RORα mRNA levels (*m+hROR*) using primers that recognize the mouse and human RORs. *E*, Q-RT-PCR analysis of mouse RORα (*mROR*) that measure the levels of the endogenous ROR mRNA levels. *F*, Northern analysis of the endogenous mouse RORα as reported previously. *G*, Q-RT-PCR analysis of mouse RORγ that measure the levels of the endogenous ROR mRNA levels. Specific primer sequences and PCR conditions are described under "Materials and Methods."

TABLE I
Key target genes in this study

ABCA1 and ABCG8	ATP-binding cassette. Transporters that transfer cholesterol to the HDL acceptors, *i.e.* reverse cholesterol efflux
ACS4	Acyl-CoA synthetase-4. Enhances the uptake of fatty acids by catalyzing their activation to acyl-CoA esters for subsequent use in catabolic fatty acid oxidation pathways
ADRP/adipophilin	Adipocyte differentiation-related protein. Involved in lipid storage
AdipoR1 and -R2	Adiponectin receptors 1 and 2. Cell surface membrane receptors for adiponectin that regulate glucose uptake and fatty acid oxidation (54)
ApoE	Apolipoprotein E. Facilitates cholesterol and lipid efflux
CAV-3	Caveolin-3. Muscle-specific caveolin involved in membrane protein anchoring, caveolae, t-tubule formation, and lipid trafficking
CPT-1	Carnitine palmitoyltransferase-1. Transfers the long chain fatty acyl group from coenzyme A to carnitine, the initial reaction of mitochondrial import of long chain fatty acids, and their subsequent oxidation
FAS	Fatty-acid synthase. Involved in *de novo* fatty acid production
FAT/fatty acid translocase and FABP3	Fatty acid translocase and fatty acid binding protein. Facilitates uptake of long chain fatty acids and low density lipoproteins
GLUT4 and -5	Glucose transporters. GLUT4 facilitates glucose uptake in response to insulin stimulation. GLUT5 catalyzes uptake of fructose
Glycogenin/GYG1	Initiates the synthesis of glycogen, the principal storage form of glucose in skeletal muscle
LPL	Lipoprotein lipase. Hydrolysis of lipoprotein triglycerides into free fatty acids and responsible for the uptake of free fatty acids
PDK-2 and -4	Pyruvate dehydroxygenase kinases. Inhibit the pyruvate dehydroxygenase complex, thereby controlling glucose oxidation and maintaining pyruvate for gluconeogenesis
SCD-1 and -2	Stearoyl-CoA desaturase-1 and -2. Enzymes associated with adiposity, *i.e.* storage and esterification of cholesterol and responsible for the cis saturation of stearoyl and palmitoyl-CoA converting them to oleate and palmitoleate, which are the monounsaturated fatty acids of triglycerides
SREBP-1c	Sterol regulatory element binding protein-1c, the hierarchical transcriptional activator of lipogenesis
UCP-1, -2 and -3	Uncoupling proteins. Mitochondrial proteins that uncouple metabolic fuel oxidation from ATP synthesis, regulating energy expenditure

analysis of critical genes (>12) involved in lipid and carbohydrate metabolism revealed similar responses to quadriceps tissue from agonist-treated C57BL/6J mice (21–23). The physiological validation of the cell culture model with respect to lipid homeostasis in the mouse corroborates the utility of this model system. This evidence, coupled to the flexibility and utility of cell culture in terms of manipulation, RNA extraction, and target validation provides an ideal platform to identify the RORα-dependent regulation of genes involved in metabolism. In addition and more importantly, we have demonstrated this cell line expresses RORα and -γ receptors and that the stable cell line produced by ectopic RORΔE overexpression has compromised endogenous RORα/γ expression and function.

We isolated total RNA from the native (wild type) and RORΔDE-differentiated myotubes, and we analyzed the expression levels of several myogenic mRNAs by quantitative real time PCR. We demonstrated as reported previously (19) that these cells retain the potential to differentiate (although

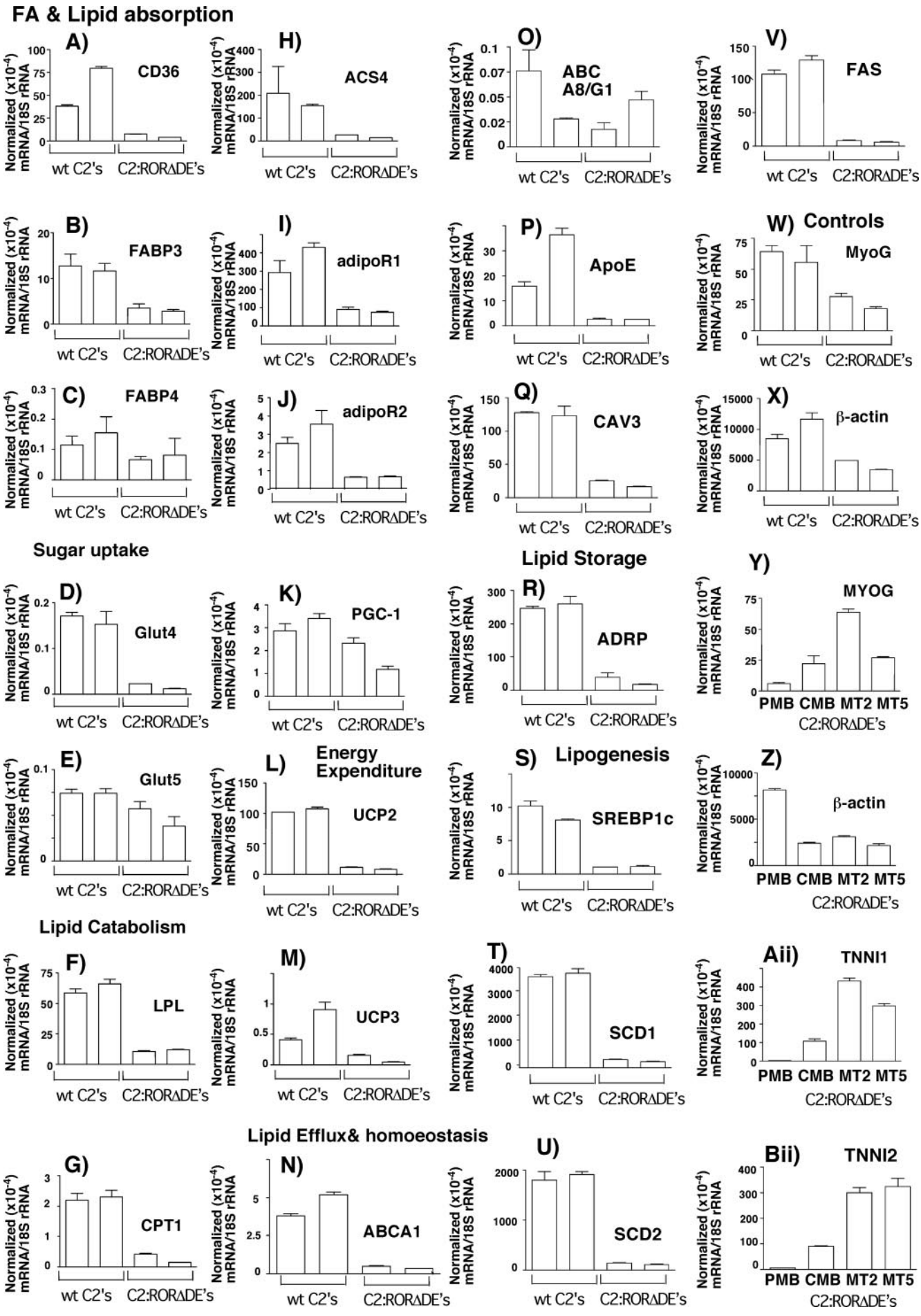

the initial rate is impaired slightly), exit the cell cycle, and express all genes associated with contraction and lipid metabolism (data not shown). This suggests that ectopic RORΔDE expression does not significantly affect proliferation, cell cycle withdrawal, differentiation, and/or phenotypic acquisition of these skeletal muscle cells.

Subsequently, we utilized quantitative real time PCR to investigate the expression pattern of genes involved in fatty acid and lipid absorption (fatty acid translocase (FAT/CD36), fatty acid binding proteins 3 and 4 (FABP3 and -4), triglyceride hydrolysis (lipoprotein lipase (LPL)), and fatty acid oxidation (muscle-type carnitine palmitoyltransferase-1 (M-CPT-1), acyl-CoA synthetase-4 (ACS-4), adiponectin receptors 1 and 2), glucose/fructose absorption, and utilization (glucose transporters 4, and 5 (GLUT4 and -5)), in total RNA isolated from C2C12 and C2:RORΔE myotubes differentiated for 5 days.

In the context of lipid and fatty acid uptake, we observed significant repression of the mRNAs encoding fatty acid translocase (FAT/CD36), and fatty acid binding protein 3 (FABP3), with only minor changes observed for fatty acid binding protein 4 (FABP4) in the RORΔE-expressing cell line, respectively (Fig. 4, *A–C*).

The transcripts encoding lipoprotein lipase, M-CPT-1, and acyl-CoA synthetase-4 (ACS-4), which are involved in triglyceride-hydrolysis, fatty acid-oxidation, and preferential fuel utilization, were significantly repressed ~5–7-fold in the RNA isolated from the cell line overexpressing RORΔE (Fig. 4, *F–H*). The significance of the repression is highlighted by the observation that expression of PPAR-γ coactivator-1 (PGC-1) mRNA (Fig. 4*K*), myogenin (myoG) mRNA (Fig. 4*W*) (which encodes the hierarchical bHLH regulator), and β-actin mRNA(Fig. 4*X*) was reduced ~2-fold. Moreover, the changes observed are not due to the effects of RORΔE expression on differentiation. Over a 5-day period the cell line retained the potential to differentiate as measured by the induction and activation of myoG (Fig. 4*Y*), troponin I slow ((TNNI1) Fig. 4*A*(*ii*)), troponin I fast ((TNNI2) (Fig. 4*B*(*ii*)), and repression of β-actin (Fig. 4*Z*) mRNA expression, respectively, after serum withdrawal.

Most interestingly, the adiponectin receptors 1 and 2 that mediate increased AMP kinase levels, as well as fatty acid oxidation and glucose uptake by adiponectin, were significantly repressed (Fig. 4, *I* and *J*). This correlates with the significant repression of glucose transporter 4 (GLUT4) mRNA expression but not glucose transporter 5 (GLUT5) mRNA (Fig. 4, *D* and *E*). However, we note that these cell lines express very low levels of the glucose transporters 4/5 (GLUT4/5) transcripts.

Subsequently, we examined the expression of genes involved in fatty acid and lipid absorption, lipid and cholesterol efflux (ATP binding cassette A1 and G1 (ABCA1/G1) and apoE), lipid storage, homeostasis (adipophilin/adipocyte differentiation-related protein (ADRP) and caveolin-3 (Cav-3)), lipogenesis ((SREBP-1c), fatty-acid synthase (FAS), stearoyl-CoA desaturase-1 and -2 (SCD-1 and -2; Fig. 4*B* and Fig. 4*E*)), and energy expenditure (uncoupling protein-1, -2, and -3 (UCP-1, -2, and -3)).

In the two polyclonal populations of cells expressing RORΔE dramatic repression, we observed dramatic reduction in the expression of mRNAs encoding ATP-binding cassette A1 (ABCA1) and apoE but minor/subtle changes in ATP-binding cassette A8/G1 (ABCA1/G1) levels (Fig. 4, *N–P*). Most interestingly, we observed significantly decreased levels of the mRNA encoding caveolin-3 (Cav-3) (Fig. 4*Q*), the major structural protein of caveolae in skeletal muscle, which has been implicated in cholesterol homeostasis. Similarly, we observed reduced expression of ADRP mRNA, a protein involved in lipid droplet formation. (Fig. 4*R*). The mRNAs encoding the hierarchical regulator of lipogenesis, SREBP-1c (Fig. 4*S*), and the lipogenic genes (SCD-1 and -2 and FAS) (Fig. 4, *T–V*) were all notably reduced in the RORΔDE-expressing cell lines. Furthermore, the mRNAs encoding UCP-2 and -3, which encode uncoupling proteins involved in energy uncoupling/expenditure and preferential lipid utilization, were significantly repressed by the expression of ectopic dominant negative RORα (Fig. 4, *L* and *M*).

Finally, the expression of the closely related but opposingly acting orphan receptors, Rev-erbα and Rev-erbβ/RVR, was further repressed by RORΔE expression (Fig. 5, *A* and *B*). This was expected as RORα has been demonstrated to regulate the Rev-erbα gene.

PGC-1 Efficiently Coactivates the Synthetic and Native RORE Heterologous Reporter Genes—We then investigated the ability of ROR to activate the synthetic and wild type ROR-dependent reporter in COS-1 cells and the ability of the cofactors p300, SRC-2/GRIP-1, and PGC-1 to coactivate ROR-dependent activation of gene expression. We utilized the synthetic RORE x5-tk-LUC reporter that contains five copies of a consensus binding site (24) and the native mPCP-2x4-tk-LUC containing four copies of the mouse Purkinje cell protein-2 RORE motif (25) cloned upstream of the heterologous herpes simplex virus thymidine kinase (tk) promoter linked to the luciferase reporter gene, respectively. As shown, RORα expression efficiently activated the expression of the synthetic (Fig. 6*A*) and native RORE (Fig. 6*B*)-containing reporters in COS-1 cells several hundredfold. In contrast, RORα relatively insignificantly (*i.e.* <10-fold) regulated the basal tk-LUC-backbone, lacking the RORE (Fig. 6*C*).

Furthermore, we observed that RORα-dependent activation of the synthetic RORE was significantly enhanced by the coactivator, PGC-1, relative to p300 and SRC-2/GRIP-1. Similarly, ROR-dependent activation of the native RORE was most efficiently coactivated by PGC-1, relative to p300 and SRC-2/GRIP-1. In summary, we demonstrate that PGC-1 expression

Fig. 4. **Expression profiling of mRNAs involved in metabolism by Q-RT-PCR analyses of the wild type native C2C12 cells and the C2:RORΔDE stably transfected cells.** Q-RT-PCR analysis of endogenous mRNA expression encoding enzymes/proteins involved in lipid homeostasis, energy expenditure, etc. (described in Table I) in two independent populations of native/wild type (*wt*) differentiated mouse C2C12 cells, and two independent polyclonal pools of the C2C12 cells stably transfected with the dominant negative human RORa1ΔDE expression vector, after 5 days of serum withdrawal are shown. These cells were denoted as wt C2s, and C2:RORΔDE, respectively. Levels of 18 S were measured in all samples; the results were normalized and presented as the number of target transcripts per 18 S transcript. For example, β-actin is equivalently expressed to 18 S. *A–C*, Q-RT-PCR analysis of mRNA expression encoding proteins/enzymes involved in lipid absorption that are completely described in Table I. *A*, fatty acid translocase (CD36/FAT); *B*, fatty acid binding protein 3 (FABP3); and *C*, FABP4. *D* and *E*, Q-RT-PCR analysis of mRNA expression encoding proteins/enzymes involved in glucose uptake that are completely described in Table I. *D*, GLUT4; *E*, GLUT5. *F–K*, Q-RT-PCR analysis of mRNA expression encoding proteins/enzymes involved in lipid catabolism that are completely described in Table I. *F*, LPL; *G*, CPT-1; *H*, ACS-4; *I* and *J*, adiponectin receptors 1 and 2 (adipoR1 and R2); *K*, PGC-1. *L* and *M*, Q-RT-PCR analysis of mRNA expression encoding proteins/enzymes involved in energy expenditure that are completely described in Table I. *L*, UCP-2; *M*, UCP-3. *N–R*, Q-RT-PCR analysis of mRNA expression encoding proteins/enzymes involved in lipid efflux and storage that are completely described in Table I. *N*, ABCA1; *O*, ABCA8/G1; *P*, apoE; *Q*, Cav-3; *R*, ADRP. *S–V*, Q-RT-PCR analysis of mRNA expression encoding proteins/enzymes involved in lipogenesis that are completely described in Table I. *S*, SREBP-1c; *T*, SCD-1; *U*, SCD-2; *V*, FAS. *W–Z*, *Aii*, and *Bii*, Q-RT-PCR analysis of mRNA expression encoding proteins associated with differentiation of the C2:RORΔDE cell line, *i.e.* MyoG, β-actin, TNNI1, and TNNI2. *W*, MyoG; *X*, β-actin; *Y*, MyoG; *Z*, β-actin; *Aii*, TNNI1; *Bii*, TNNI2.

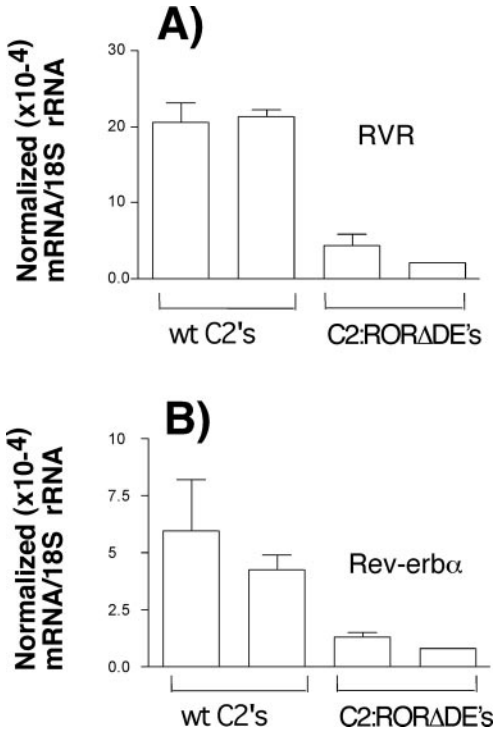

FIG. 5. **Q-RT-PCR analyses of orphan nuclear receptor expression in the hRORΔDE stably transfected C2C12 cell line.** Q-RT-PCR analysis of endogenous mRNAs encoding the closely related Rev-erb and RVR orphan nuclear receptors in two independent populations of native/wild type (*wt*) differentiated mouse C2C12 cells and two independent polyclonal pools of the C2C12 cells stably transfected with the dominant negative human RORΔDE expression vector, after 5 days of serum withdrawal, are shown. These cells were denoted as wt C2s and C2:RORΔDE, respectively. Q-RT-PCR analyses of RVR mRNA expression (*A*) and Rev-erbα mRNA expression (*B*) in wt C2s and C2:RORΔDE cells. Specific primer sequences and conditions for RVR and Rev-erb Q-RT-PCR are described under "Materials and Methods." Levels of 18 S were measured in all samples, and the results are presented as number of target transcripts per 18 S transcript. For example β-actin is equivalently expressed to 18 S.

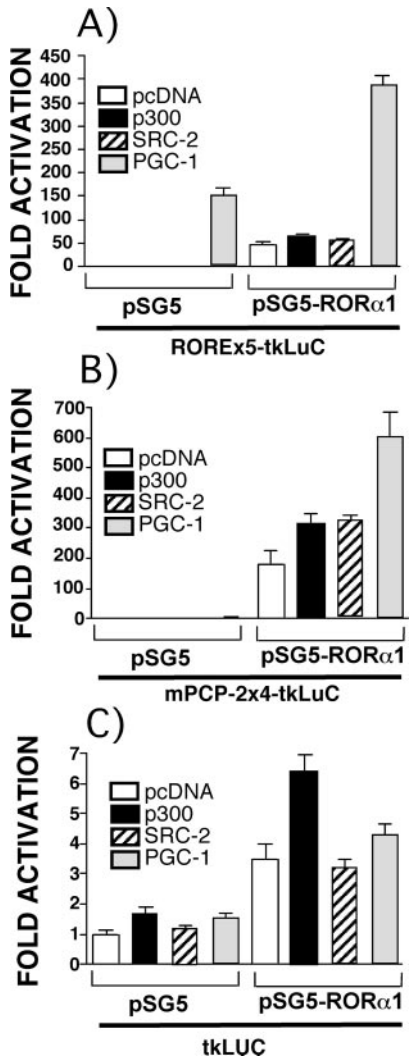

FIG. 6. **PGC-1 acts as a transcriptional coactivator for ROR-mediated activation of the heterologous synthetic and native RORE reporter genes.** *A*, each well of a 24-well plate of COS-1 cells (~60% confluence) was cotransfected with 0.33 μg of the synthetic reporter (*i.e.* the ROREx5-tk-LUC containing five copies of the TATAT-CAAGGTCAT sequence), 0.33 μg of either pSG5 or pSG5-RORα1, and 0.1 μg of pcDNA expression vectors encoding p300, SRC-2/GRIP-1, and PGC-1 (*i.e.* a total of ~0.7 μg of DNA per well) by using the liposome-mediated transfection procedure as described previously. Fold activation is expressed relative to LUC activity obtained after cotransfection of the reporter and vector only, arbitrarily set at 1. The mean fold activation values and S.D. (*bars*) were derived from a minimum of two independent experiments composed of six replicates. *B*, each well of a 24-well plate of COS-1 cells (~60% confluence) was cotransfected with 0.33 μg of the native reporter (*i.e.* the mouse PCP-2x4-tk-LUC contains four copies of the native sequence GTTATAGTAACTGGGTCAGGG-GACT), 0.33 μg of either pSG5 or pSG5-RORα1, and 0.1 μg of pcDNA expression vectors encoding p300, SRC-2/GRIP-1, and PGC-1.(*i.e.* a total of ~0.7 μg DNA per well) using the liposome-mediated transfection procedure as described. *C*, each well of a 24-well plate of COS-1 cells (~60% confluence) was cotransfected with 0.33 μg of the tk-LUC vector, 0.33 μg of either pSG5 or pSG5-RORα1, and 0.1 μg of pcDNA expression vectors encoding p300, SRC-2/GRIP-1, and PGC-1 (*i.e.* a total of ~0.7 μg of DNA per well) by using the liposome-mediated transfection procedure as described previously and above.

selectively coactivates RORα-mediated activation of the heterologous synthetic and native RORE-tk-LUC reporters.

M-CPT-1 and Cav-3 Genes Are Primary Targets of RORα in Skeletal Muscle—We further explored the molecular basis of ROR-mediated gene activation in skeletal muscle cells by evaluating whether direct or indirect mechanisms mediated the observed changes in mRNA levels in the RORΔDE cells. We investigated the responsiveness of the promoters of selected target genes to RORα coexpression in a cell-based reporter assay.

We transiently transfected COS-1 cells with the regulatory sequences of selected target genes, including ABCA1 (22), CD36/FAT (37), LPL (38), M-CPT-1 (26), Cav-3, GLUT4, and UCP-2 (39), cloned in front of the pGL2/3 basic luciferase backbone, and we examined the response after cotransfection of RORα in the presence and absence of p300, SRC-2/GRIP-1, and PGC-1.

Most interestingly, the M-CPT-1 promoter (and not several other promoters including GLUT4), which contains 1025 bp upstream of the start of translation, was efficiently activated by ROR expression (Fig. 7*A*). Moreover, we observed that p300 and PGC-1 significantly enhanced the transactivation of the M-CPT-1 (Fig. 7*B*). The transcriptional coactivators p300 and PGC-1 are expressed in skeletal muscle and have been demonstrated to potentiate myogenesis, mitochondrial biogenesis, oxidative metabolism, fiber type transitions (fast (type II) to slow (type I)), and thermogenesis. Furthermore, we observed similar ROR-dependent activation and cofactor preference with a VP16-RORα chimera (Fig. 7*C*). Most interestingly, the p-mCav3–2595-LUC promoter that encompasses 2595 bp immediately upstream of the murine Cav-3 transcription start site (that drives the expression of the muscle-specific caveolin-3 gene) was also efficiently activated by RORα expression (Fig. 8*A*).

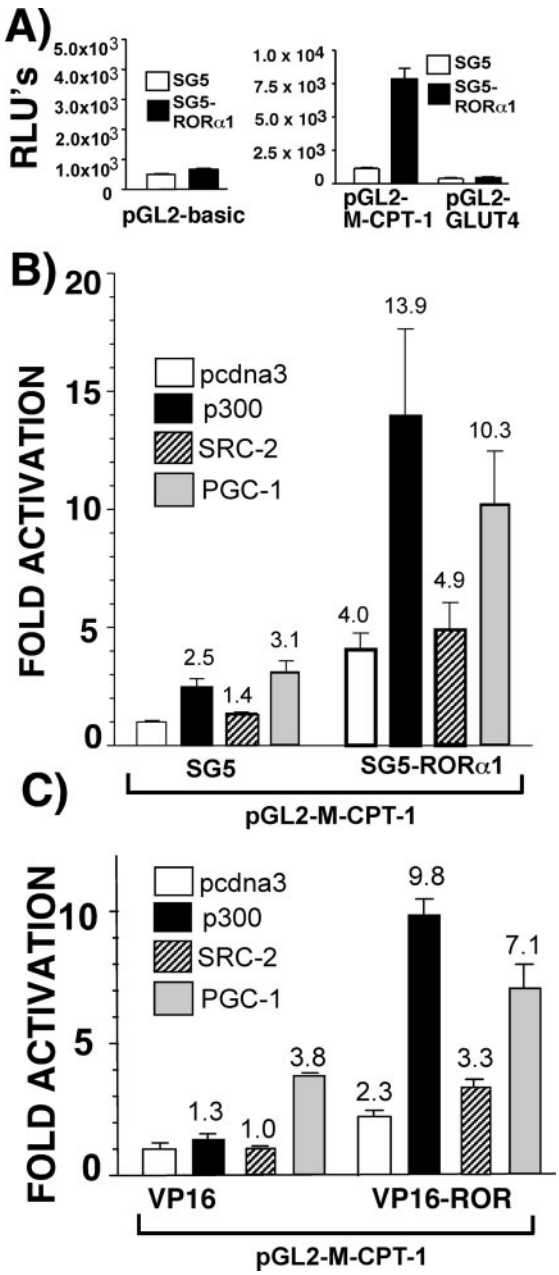

FIG. 7. **The M-CPT-1 promoter is directly activated by ROR and coactivated by p300 and PGC-1.** *A*, each well of a 24-well plate of COS-1 cells (~60% confluence) was cotransfected with either 0.33 μg of pGL2-basic, pGL2-MCPT1$_{(-1025/-12)}$, or pGL2-GLUT4, and 0.33 μg of either pSG5 or pSG5-RORα1 (*i.e.* a total of ~0.66 μg of DNA per well) by using the liposome-mediated transfection procedure as described previously and above (Fig. 6*A*). *B*, each well of a 24-well plate of COS-1 cells (~60% confluence) was cotransfected with 0.33 μg of pGL2-MCPT1$_{(-1025/-12)}$, 0.33 μg of either pSG5 or pSG5-RORα1, and 0.1 μg of pcDNA expression vectors encoding p300, SRC-2/GRIP-1, and PGC-1 (*i.e.* a total of ~0.7 μg of DNA per well) using the liposome-mediated transfection procedure as described. *C*, each well of a 24-well plate of COS-1 cells (~60% confluence) was cotransfected with 0.33 μg of pGL2-MCPT1$_{(-1025/-12)}$, 0.33 μg of either VP16 vector alone or the VP16-RORα1 chimera, and 0.1 μg of pcDNA expression vectors encoding p300, SRC-2/GRIP-1, and PGC-1.(*i.e.* a total of ~0.66 μg of DNA per well) by using the liposome-mediated transfection procedure as described.

In an attempt to further elucidate which sequences were necessary for the trans-activation of the mCav-3-LUC promoter by RORα, we utilized a series of 5′ unidirectional deletions in the mCav-3 promoter. Several deletion constructs were produced, namely p-mCav3–988-LUC, p-mCav3–654-LUC, p-mCav3–477-LUC, and p-mCav3–279-LUC, which contained 988, 654, 477, and 279 nucleotides, respectively, of 5′-flanking sequences cloned upstream of the luciferase reporter in pGL2-Basic. By transfecting the full-length and deleted promoters in the absence/presence of the RORα expression vector in COS-1 cells, we could demonstrate that the sequences between nucleotide position −2595 and −988 were necessary for RORα-dependent activation (Fig. 8*A*). Moreover, we observed that p300 and SRC-2/GRIP-1 significantly enhanced the transactivation of the mCav-3 promoter. (Fig. 8*B*).

To define rigorously the molecular basis of direct ROR action, we focused on one of the promoters that we defined as a primary ROR target gene. We selected and scanned the mouse caveolin-3 promoter by the Mat inspector program to identify putative AGGTCA nuclear receptor binding motifs. We observed six putative ROR monomeric binding motifs m1–m6, located between nucleotide positions −2498/−2474, 2378/−2357, −1739/−1713, −1720/−1690, −1587/−1556, and −1005/−984, respectively (Fig. 8*C*). These motifs to varying degrees could be accommodated by the asymmetric (A/T)$_6$RGGTCA ROR recognition motif and were located in the delimited region between nucleotide positions −2595 and −988 that were necessary for RORα-dependent activation.

Subsequently, we examined the ability of the motifs 1–6 to interact with GST-ROR, and we observed that motifs 2 and 4–6 bound ROR with different efficiencies in an EMSA assay, relative to our control ROR recognition motif, the mouse PCP-2 RORE (Fig. 8*D*). However, we observed that only the m2 and m6 (and the synthetic RORE), but not the m1 and M3–M5 motifs) efficiently competed against the efficient GST-ROR-mPCP-2 RORE interaction (Fig. 8*E*). This suggested that either motif 2 or 6 mediated ROR activation of the mouse caveolin-3 gene. Hence, we independently mutated the GG nucleotide in the nuclear receptor half-sites to TT in the m2 and m6 putative ROREs within the native caveolin-3 promoter, and we examined the ability of ROR (in the presence of the cofactor p300) to trans-activate the caveolin-3 promoter. We observed that the mutation of motif 6 in the mouse caveolin-3 promoter compromised the ability of ROR to trans-activate the promoter (Fig. 8*F*). This was also consistent with the analysis of several additional 5′ unidirectional deletion mutants of the caveolin-3 promoter between −2595 and −984 that were examined (data not shown).

In summary, these transfections demonstrated that RORα directly regulates the CPT-1 and Cav-3 genes that potentially encode proteins involved in β-oxidation and cholesterol homeostasis. Moreover, we defined the specific sequences in a muscle-specific gene (*i.e.* caveolin-3) that mediated the direct regulation of expression by ROR. This suggests that RORα has a central role in the regulation of lipid homeostasis.

DISCUSSION

Genetic, molecular, and biochemical studies have demonstrated that NR1F1 (RORα)-deficient mice develop severe atherosclerosis, low HDL-C, hypo-α-lipoproteinemia, muscular atrophy, and heightened inflammatory responses. Moreover, NR1F1 regulates the expression of apolipoprotein CIII, a component of HDL and very low density lipoprotein that plays a role in regulation of triglyceride levels and lipoprotein lipase activity. Furthermore, RORα potentiates the acquisition of the skeletal muscle phenotype.

The expression of RORα in skeletal muscle, a peripheral lean tissue that has a significant role in energy consumption, glucose disposal, and free fatty acid uptake prompted us to investigate the regulatory role of RORα in skeletal muscle cells, with respect to gene expression involved in metabolism. Our study demonstrates that RORα regulates the expression of genes

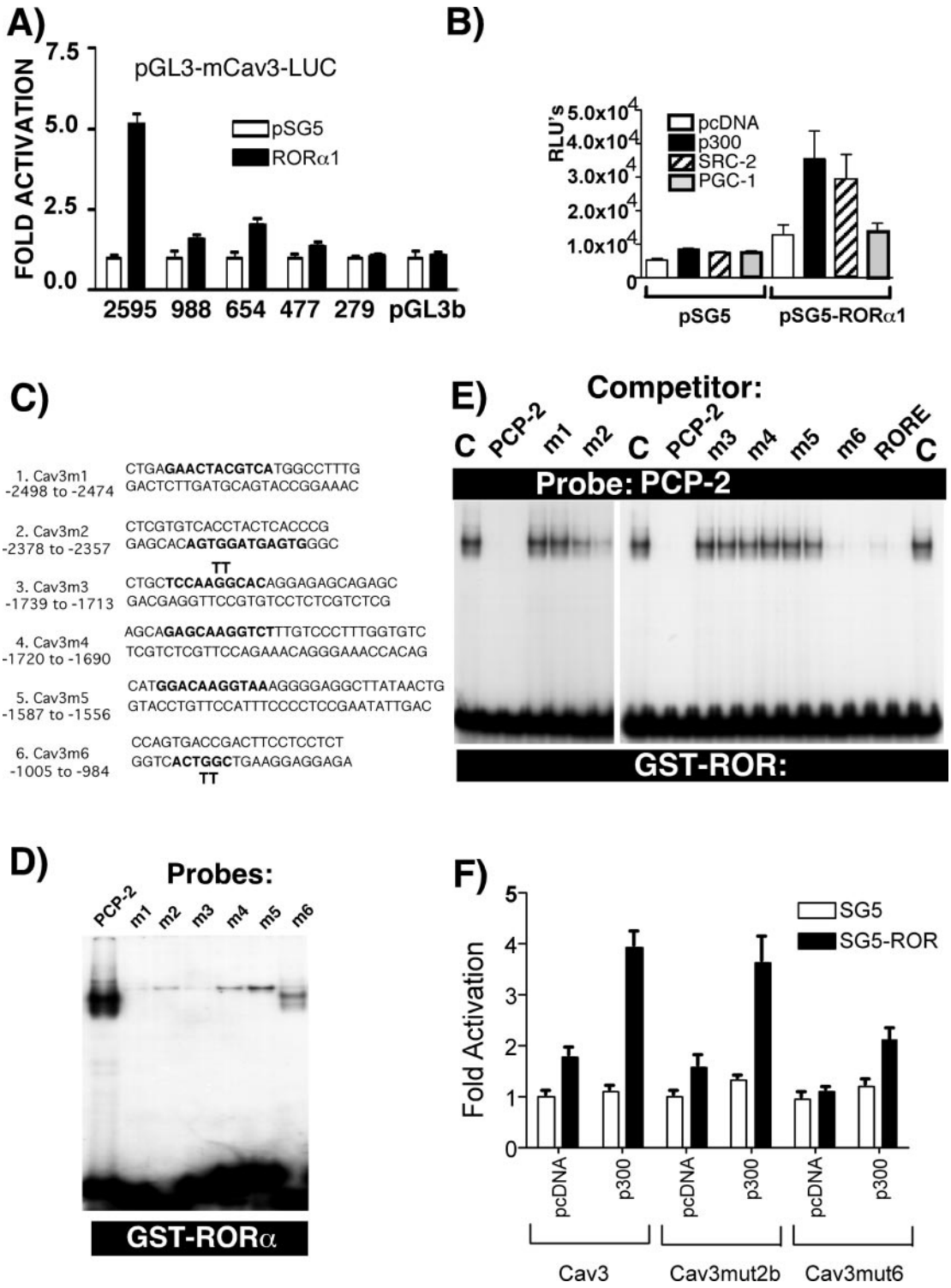

FIG. 8. **The caveolin-3 promoter is directly activated by RORα and coactivated by p300 and SRC-2.** *A*, each well of a 24-well plate of COS-1 cells (~60% confluence) was cotransfected with either 0.33 μg of pGL3-basic and a series of mouse pGL3-mCav3 promoter deletions −2595/+35 (*2595*), −988/+35 (*988*), −654/+35 (*654*), −477/+35 (*477*), −279/+35 (*279*), and 0.33 μg of either pSG5 or pSG5-RORα1 (*i.e.* a total of ~0.66 μg of DNA per well) using the liposome-mediated transfection procedure as described above. *B*, each well of a 24-well plate of COS-1 cells (~60% confluence) was cotransfected with 0.33 μg of pGL3-mCav3-LUC (−2595/+35), 0.33 μg of either pSG5 or pSG5-RORα1, and 0.1 μg of pcDNA expression vectors encoding p300, SRC-2/GRIP-1, and PGC-1.(*i.e.* a total of ~0.7 μg of DNA per well) by using the liposome-mediated transfection procedure as described above. *C*, sequence of putative RORE motifs (in *boldface*) identified in the mouse caveolin-3 promoter. *TT below the line* denotes mutagenesis of the bases above from GG to TT by QuickChange site-directed mutagenesis referred to in *F*. *D*, EMSA analysis examining the differential interaction of the six putative RORE motifs in the caveolin-3 promoter (denoted as Cav-3 motifs (*m*) 1–6) with GST-RORα1. 300 cps of PAGE-purified, ^{32}P-end radiolabeled Cav-3 m1–6 were incubated with 0.4 μg of GST-RORα1 protein before PAGE separation. The mPCP-2 radiolabeled probe was used as a positive control (see "Materials and Methods"). *E*, EMSA analysis examining the ability of the six putative m1–6 ROREs (at 10- and 30-fold excess) to efficiently compete the mPCP-2·ROR complex. ^{32}P-Radiolabeled mouse PCP-2 RORE probe was coincubated with 0.4 μg of GST-RORα1 protein, and 100 and 300 ng of unlabeled putative Cav-3 m1–6 ROREs before PAGE separation. Cold mPCP-2 and synthetic ROREs were used as the control competitors (see "Materials and Methods"). *F*, each well of a 24-well plate of COS-1 cells (~60% confluence) was cotransfected with 0.4 μg of pGL3-mCav3-LUC (−2595/+35) or pGL3-mCav3-LUC (−2595/+35) carrying the GG to TT mutations in motifs 2 and 6 (see *C*) in the presence 0.1 μg of pcDNA or pcDNA-p300 and 0.16 μg of pSG5 or pSG5-RORα1 as described under "Materials and Methods."

involved in lipid absorption, β-oxidation, cholesterol efflux, and energy expenditure in skeletal muscle cells. The observed changes in gene expression in skeletal muscle are consistent with the phenotype in this animal model.

The natural RORα mouse mutant, called *staggerer* (*sg/sg*), is susceptible to high fat diet-induced atherosclerosis, with atherosclerotic lesions in the aorta and the large and small coronary arteries. In the context of this investigation, the *staggerer* mice exhibit an aberrant blood lipid profile with lower circulating plasma levels of HDL-C (associated with decreased plasma apoA-I and apoA-II), reduced apoCIII, and plasma triglycerides. Decreases in specific lipoprotein compartments, namely apoAI, the major constituent of HDL, and apoAII, leads to a pronounced hypo-α-lipoproteinemia (16). Accordingly, it has been shown that RORα regulates the expression of apoAI and apoCIII in cell culture (16, 17). Further studies in *staggerer* mice correlate atherogenic susceptibility in this animal model to a complex phenotype that includes aberrant vascular physiology, lipid profiles, and inflammatory responses. However, the contribution of skeletal muscle (atrophied in the RORα *sg/sg* mice) and other putative target tissues to the *staggerer* phenotype has not been resolved. Finally, RORα target genes and the mechanism of action in this metabolically demanding major mass lean tissue remained unclear.

The study by Mamontova *et al.* (40) demonstrated the RORα *sg/sg* mice have lowered plasma HDL cholesterol. We demonstrate that the muscle cells with attenuated RORα expression and function display decreased ABCA1 mRNA expression. Furthermore, we demonstrated that muscle-specific caveolin-3 mRNA expression is compromised in the cell line expressing RORΔDE. In addition, we demonstrated that the caveolin-3 gene is a direct RORα target in muscle cells. Whereas caveolin-3 has not been directly linked to lipid regulation, studies of the non-muscle caveolin family member, caveolin-1, have suggested a role for caveolins in cholesterol transport to extracellular cholesterol acceptors such as HDL; increased caveolin-1 expression increases cholesterol efflux to extracellular acceptors. Furthermore, apoA-I and cholesterol acceptor availability regulates caveolin-1 expression (41, 42). Nonstriated muscle caveolins have also been linked to other aspects of lipid regulation; caveolin-1 and -2 associate with lipid droplets in a fatty acid-regulated fashion in cultured cells and *in vivo* (43). Moreover, caveolin-1 null mice are resistant to diet-induced obesity (44) and show defective lipid droplet formation in a model system (56). Recent studies (45) showed that caveolin-1 expression increases, and caveolin-2 expression decreases, in white adipose tissue from rodents on a high fat diet. The studies presented here linking RORα to the regulation of caveolin-3 and ADRP mRNA expression raises the intriguing possibility that, like the non-muscle caveolins, caveolin-3 may play a role in lipid regulation. This is consistent with studies showing that a caveolin-3 mutant associates with lipid droplets and can perturb the cellular balance of neutral lipids and free cholesterol in cultured cells (43, 46).

We further observed in the cell line expressing ectopic dominant negative RORα that expression of genes involved in lipid absorption, lipid catabolism, lipogenesis, and energy expenditure was significantly repressed. This provides further evidence that RORα is a critical regulator of lipid homeostasis. Moreover, the repression of SREBP-1c expression and its target genes (for example, FAS, SCD-1, and -2) in the muscle cell line expressing the truncated RORα, similar in size and function to the form in the *staggerer* mouse, is consistent with the reduced plasma triglycerides observed in this animal model. In addition the *staggerer* mouse has lower apoCIII expression in the liver, which affects lipoprotein metabolism.

The neural degeneration and motor and coordination (*i.e.* spatial memory) abnormalities in *staggerer* mice are consistent with the aberrant lipid metabolism observed. Defects in β-oxidation and lipid turnover are associated with neurologic disease (47).

We demonstrate that RORα has a significant role in the regulation of the mRNAs encoding the uncoupling proteins (UCP-2 and -3, mitochondrial proton carriers) that control metabolic efficiency, energy expenditure, and thermogenesis by uncoupling an oxidation/respiration-induced proton gradient from ATP synthesis. The repression of UCP mRNA expression correlates and is in concordance with the decreased mRNA expression of genes involved in absorption and utilization of lipids and fatty acids. For example, reduced lipoprotein lipase activity in skeletal muscle results in decreased UCP-3 mRNA expression, consistent with the hypothesis that it regulates the flux of lipid substrates across the mitochondria. Moreover, inhibition of fatty acid oxidation leads to reduced UCP-2 and -3 mRNA expression in slow twitch oxidative muscle fibers. *staggerer* mice are lean despite their hyperphagia (like Cav-1 mice). The lean phenotype may correlate with the decreased levels of SCD-1 and -2 mRNA observed, although increased brown adipose tissue activity may account for this phenotype.

In addition, we demonstrate that M-CPT-1, an established target for PPARα in cardiac muscle (26, 48, 49) and PPARβ/δ in skeletal muscle cells, is also directly regulated by RORα and coactivated by p300 and PGC-1. Moreover, it suggests crosstalk may occur between PPAR and RORα signaling in a tissue-specific manner.

The fact that RORα is involved in all of these processes highlights the crucial role of RORα in lipid homeostasis and identifies RORα as a promising therapeutic target in the treatment of dyslipidemia. Skeletal muscle is rapidly emerging as a critical target tissue in the battle against obesity, type II diabetes, dyslipidemia, syndrome X, and atherosclerosis. For example, NRs in skeletal muscle, such as LXR, PPARα, -β/δ, and -γ, have been shown to be involved in enhancing the insulin-stimulated glucose disposal rate, decreasing triglycerides, and increasing lipid catabolism, cholesterol efflux, and plasma HDL-C levels (21–23). Hence, orphan NRs (for example ROR) that regulate lipid and carbohydrate metabolism, energy expenditure, and thermogenesis in skeletal muscle have enormous pharmacological utility for the treatment of dyslipidemia and syndrome X. In conclusion, we suggest that ROR in skeletal muscle cells programs a cascade of gene expression designed to regulate lipid homeostasis. We hypothesize that RORα is a critical regulator of lipid and energy homeostasis in this major mass of lean tissue. Moreover, we suggest that the atherogenic and dyslipidemic phenotype of the *staggerer* mouse is related to aberrant RORα function in skeletal muscle. Finally, we surmise that ROR agonists may have therapeutic utility in the treatment of hypercholesterolemia, atherosclerosis, and obesity.

REFERENCES

1. Green, S., and Chambon, P. (1988) *Trends Genet.* **4,** 309–314
2. Evans, R. M. (1988) *Science* **240,** 889–895
3. Adelmant, G., Begue, A., Stehelin, D., and Laudet, V. (1996) *Proc. Natl. Acad. Sci. U. S. A.* **93,** 3553–3558
4. Bonnelye, E., Vanacker, J. M., Desbiens, X., Begue, A., Stehelin, D., and Laudet, V. (1994) *Cell Growth Differ.* **5,** 1357–1365
5. Retnakaran, R., Flock, G., and Giguere, V. (1994) *Mol. Endocrinol.* **8,** 1234–1244
6. Forman, B. M., Chen, J., Blumberg, B., Kliewer, S. A., Henshaw, R., Ong, E. S., and Evans, R. M. (1994) *Mol. Endocrinol.* **8,** 1253–1261
7. Dumas, B., Harding, H. P., Choi, H. S., Lehmann, K. A., Chung, M., Lazar, M. A., and Moore, D. D. (1994) *Mol. Endocrinol.* **8,** 996–1005
8. Giguere, V., Tini, M., Flock, G., Ong, E., Evans, R. M., and Otulakowski, G. (1994) *Genes Dev.* **8,** 538–553
9. Harding, H. P., and Lazar, M. A. (1993) *Mol. Cell. Biol.* **13,** 3113–3121
10. Beckerandre, M., Andre, E., and Delamarter, J. F. (1993) *Biochem. Biophys. Res. Commun.* **194,** 1371–1379

11. Carlberg, C., Vanhuijsduijnen, R. H., Staple, J. K., Delamarter, J. F., and Beckerandre, M. (1994) *Mol. Endocrinol.* **8,** 757–770
12. Hirose, T., Smith, R. J., and Jetten, A. M. (1994) *Biochem. Biophys. Res. Commun.* **205,** 1976–1983
13. Ortiz, M. A., Piedrafita, F. J., Pfahl, M., and Maki, R. (1995) *Mol. Endocrinol.* **9,** 1679–1691
14. Carlberg, C., and Wiesenberg, I. (1995) *J. Pineal Res.* **18,** 171–178
15. Vosper, H., Khoudoli, G. A., Graham, T. L., and Palmer, C. N. (2002) *Pharmacol. Ther.* **95,** 47–62
16. Raspe, E., Duez, H., Gervois, P., Fievet, C., Fruchart, J. C., Besnard, S., Mariani, J., Tedgui, A., and Staels, B. (2001) *J. Biol. Chem.* **276,** 2865–2871
17. Vu-Dac, N., Gervois, P., Grotzinger, T., De Vos, P., Schoonjans, K., Fruchart, J. C., Auwerx, J., Mariani, J., Tedgui, A., and Staels, B. (1997) *J. Biol. Chem.* **272,** 22401–22404
18. Steinmayr, M., Andre, E., Conquet, F., Rondi-Reig, L., Delhaye-Bouchaud, N., Auclair, N., Daniel, H., Crepel, F., Mariani, J., Sotelo, C., and Becker-Andre, M. (1998) *Proc. Natl. Acad. Sci. U. S. A.* **95,** 3960–3965
19. Lau, P., Bailey, P., Dowhan, D. H., and Muscat, G. E. (1999) *Nucleic Acids Res.* **27,** 411–420
20. Jarvis, C. I., Staels, B., Brugg, B., Lemaigre-Dubreuil, Y., Tedgui, A., and Mariani, J. (2002) *Mol. Cell. Endocrinol.* **186,** 1–5
21. Tanaka, T., Yamamoto, J., Iwasaki, S., Asaba, H., Hamura, H., Ikeda, Y., Watanabe, M., Magoori, K., Ioka, R. X., Tachibana, K., Watanabe, Y., Uchiyama, Y., Sumi, K., Iguchi, H., Ito, S., Doi, T., Hamakubo, T., Naito, M., Auwerx, J., Yanagisawa, M., Kodama, T., and Sakai, J. (2003) *Proc. Natl. Acad. Sci. U. S. A.* **100,** 15924–15929
22. Muscat, G. E., Wagner, B. L., Hou, J., Tangirala, R. K., Bischoff, E. D., Rohde, P., Petrowski, M., Li, J., Shao, G., Macondray, G., and Schulman, I. G. (2002) *J. Biol. Chem.* **277,** 40722–40728
23. Dressel, U., Allen, T. L., Pippal, J. B., Rohde, P. R., Lau, P., and Muscat, G. E. (2003) *Mol. Endocrinol.* **17,** 2477–2493
24. Medvedev, A., Yan, Z. H., Hirose, T., Giguere, V., and Jetten, A. M. (1996) *Gene* (*Amst.*) **181,** 199–206
25. Matsui, T. (1997) *Genes Cells* **2,** 263–272
26. Brandt, J. M., Djouadi, F., and Kelly, D. P. (1998) *J. Biol. Chem.* **273,** 23786–23792
27. Chen, S. L., Dowhan, D. H., Hosking, B. M., and Muscat, G. E. (2000) *Genes Dev.* **14,** 1209–1228
28. Puigserver, P., Wu, Z., Park, C. W., Graves, R., Wright, M., and Spiegelman, B. M. (1998) *Cell* **92,** 829–839
29. Hamilton, B. A., Frankel, W. N., Kerrebrock, A. W., Hawkins, T. L., FitzHugh, W., Kusumi, K., Russell, L. B., Mueller, K. L., van Berkel, V., Birren, B. W., Kruglyak, L., and Lander, E. S. (1996) *Nature* **379,** 736–739
30. McBroom, L. D., Flock, G., and Giguere, V. (1995) *Mol. Cell. Biol.* **15,** 796–808
31. Wade, R., Sutherland, C., Gahlmann, R., Kedes, L., Hardeman, E., and Gunning, P. (1990) *Dev. Biol.* **142,** 270–282
32. Lloyd, C., Schevzov, G., and Gunning, P. (1992) *J. Cell Biol.* **117,** 787–797
33. Brennan, K. J., and Hardeman, E. C. (1993) *J. Biol. Chem.* **268,** 719–725
34. Dunwoodie, S. L., Joya, J. E., Arkell, R. M., and Hardeman, E. C. (1994) *J. Biol. Chem.* **269,** 12212–12219
35. Shani, M. (1986) *Mol. Cell. Biol.* **6,** 2624–2631
36. Shani, M., Dekel, I., and Yoffe, O. (1988) *Mol. Cell. Biol.* **8,** 1006–1009
37. Shore, P., Dietrich, W., and Corcoran, L. M. (2002) *Nucleic Acids Res.* **30,** 1767–1773
38. Homma, H., Kurachi, H., Nishio, Y., Takeda, T., Yamamoto, T., Adachi, K., Morishige, K., Ohmichi, M., Matsuzawa, Y., and Murata, Y. (2000) *J. Biol. Chem.* **275,** 11404–11411
39. Kizaki, T., Suzuki, K., Hitomi, Y., Taniguchi, N., Saitoh, D., Watanabe, K., Onoe, K., Day, N. K., Good, R. A., and Ohno, H. (2002) *Proc. Natl. Acad. Sci. U. S. A.* **99,** 9392–9397
40. Mamontova, A., Seguret-Mace, S., Esposito, B., Chaniale, C., Bouly, M., Delhaye-Bouchaud, N., Luc, G., Staels, B., Duverger, N., Mariani, J., and Tedgui, A. (1998) *Circulation* **98,** 2738–2743
41. Hailstones, D., Sleer, L. S., Parton, R. G., and Stanley, K. K. (1998) *J. Lipid Res.* **39,** 369–379
42. Bist, A., Fielding, P. E., and Fielding, C. J. (1997) *Proc. Natl. Acad. Sci. U. S. A.* **94,** 10693–10698
43. Pol, A., Martin, S., Fernandez, M. A., Ferguson, C., Carozzi, A., Luetterforst, R., Enrich, C., and Parton, R. G. (2004) *Mol. Biol. Cell* **15,** 99–110
44. Razani, B., Combs, T. P., Wang, X. B., Frank, P. G., Park, D. S., Russell, R. G., Li, M., Tang, B., Jelicks, L. A., Scherer, P. E., and Lisanti, M. P. (2002) *J. Biol. Chem.* **277,** 8635–8647
45. Lopez, I. P., Milagro, F. I., Marti, A., Moreno-Aliaga, M. J., Martinez, J. A., and De Miguel, C. (2004) *Biochem. Biophys. Res. Commun.* **318,** 234–239
46. Pol, A., Luetterforst, R., Lindsay, M., Heino, S., Ikonen, E., and Parton, R. G. (2001) *J. Cell Biol.* **152,** 1057–1070
47. Forss-Petter, S., Werner, H., Berger, J., Lassmann, H., Molzer, B., Schwab, M. H., Bernheimer, H., Zimmermann, F., and Nave, K. A. (1997) *J. Neurosci. Res.* **50,** 829–843
48. Huss, J. M., Levy, F. H., and Kelly, D. P. (2001) *J. Biol. Chem.* **276,** 27605–27612
49. Barger, P. M., Brandt, J. M., Leone, T. C., Weinheimer, C. J., and Kelly, D. P. (2000) *J. Clin. Investig.* **105,** 1723–1730
50. Burke, L., Downes, M., Carozzi, A., Giguere, V., and Muscat, G. E O. (1996) *Nucleic Acids Res.* **24,** 3481–3489
51. Downes, M., Carozzi, A. J., and Muscat, G. E. O. (1995) *Mol. Endocrinol.* **9,** 1666–1678
52. Dowhan, D. H., Downes, M., Sturm, R. A., and Muscat, G. E. (1994) *Endocrinology* **135,** 2592–2607
53. Preitner, N., Damiola, F., Lopez-Molina, L., Zakany, J., Duboule, D., Albrecht, U., and Schibler, U. (2002) *Cell* **110,** 251–260
54. Yamauchi, T., Kamon, J., Ito, Y., Tsuchida, A., Yokomizo, T., Kita, S., Sugiyama, T., Miyagishi, M., Hara, K., Tsunoda, M., Murakami, K., Ohteki, T., Uchida, S., Takekawa, S., Waki H., Tsuno, N. H., Shibata, Y., Terauchi, Y., Froguel, P., Tobe, K., Koyasu, S., Taira, K., Kitamura, T., Shimuzu, T., Nagai, R., and Kadowaki, T. (2003) *Nature* **423,** 762–769
55. Curlewis, J. D., Tam, S. P., Lau, P., Kusters, D. H., Barclay, J. L., Anderson, S. T., and Waters, M. J. (2002) *Endocrinology* **143,** 3984–3993
56. Cohen, A. W., Razani, B., Schubert, W., Williams, T. M., Wang, X. B., Iyengar, P., Brasaemle, D. L., Scherer, P. E., and Lisanti, M. P. (2004) *Diabetes* **53,** 1261–1270

RORα Regulates the Expression of Genes Involved in Lipid Homeostasis in Skeletal Muscle Cells: CAVEOLIN-3 AND CPT-1 ARE DIRECT TARGETS OF ROR

Patrick Lau, Susan J. Nixon, Robert G. Parton and George E. O. Muscat

J. Biol. Chem. 2004, 279:36828-36840.
doi: 10.1074/jbc.M404927200 originally published online June 15, 2004
